

Two-Photon Absorption in $\text{Ca}_3(\text{VO}_4)_2$ and $\text{Ca}_{2.7}\text{Sr}_{0.3}(\text{VO}_4)_2$ Crystals

Igor O. Kinyaevskiy ^{1,*}, Valery I. Kovalev ¹, Nikita S. Semin ¹, Pavel A. Danilov ¹, Sergey I. Kudryashov ¹, Andrey V. Koribut ¹ and Elizaveta E. Dunaeva ²

¹ P.N. Lebedev Physical Institute of the Russian Academy of Sciences, 119991 Moscow, Russia

² Prokhorov General Physics Institute of the Russian Academy of Sciences, 119991 Moscow, Russia

* Correspondence: kinyaevskiyio@lebedev.ru

Abstract: Two-photon absorption has been systematically studied in $\text{Ca}_3(\text{VO}_4)_2$ and $\text{Ca}_{2.7}\text{Sr}_{0.3}(\text{VO}_4)_2$ crystals, both of which are prospective nonlinear optical and laser host materials. A strong dependence of the two-photon absorption coefficients on the orientation of the laser beam polarization with respect to the optical c-axis of the crystals is revealed. The measured coefficients for perpendicular and parallel orientations were 50 ± 10 cm/TW and 19 ± 4 cm/TW in $\text{Ca}_3(\text{VO}_4)_2$, and 18 ± 3 cm/TW and 10 ± 2 cm/TW in $\text{Ca}_{2.7}\text{Sr}_{0.3}(\text{VO}_4)_2$, respectively. Thus, to minimize optical losses caused by two-photon absorption, an orientation of $\text{Ca}_{2.7}\text{Sr}_{0.3}(\text{VO}_4)_2$ crystals with the laser beam polarization parallel to the crystal optical c-axis is preferred.

Keywords: two-photon absorption; calcium orthovanadate; $\text{Ca}_3(\text{VO}_4)_2$; $\text{Ca}_{3-x}\text{Sr}_x(\text{VO}_4)_2$; orientation effects

1. Introduction

Calcium orthovanadate $\text{Ca}_3(\text{VO}_4)_2$ attracts attention as both a promising host material for lasers [1,2] and a material for nonlinear optics [3–5]. In addition, its linear and nonlinear optical properties can be varied and optimized for particular purposes by producing solid solutions such as $\text{Ca}_{9.5-1.5x}\text{Bi}_x\text{Cd}(\text{VO}_4)_7$ [6] and $\text{Ca}_{3-x}\text{Sr}_x(\text{VO}_4)_2$ (CSVO, $x \geq 0$) [7]. One interesting feature of CSVO is that the vibrational modes in its spontaneous Raman spectrum are strongly broadened—the linewidth of the strongest mode $\nu_1 = 854 \text{ cm}^{-1}$ is $\Delta\nu = 50 \text{ cm}^{-1}$ at $x = 0$ [7,8], which is an order of magnitude higher than that in other crystals. This fact may indicate a short phase relaxation time for vibrational excitation T_2 , which makes this material interesting for the conversion of ultrashort (sub-picosecond) laser pulses via stimulated Raman scattering (SRS).

Although a recent investigation [5] demonstrated that T_2 for CSVO, $x = 0.3$, is larger than $1/\pi c \Delta\nu$ (about several picoseconds), this material demonstrated a reasonably high SRS efficiency for visible-range sub-picosecond laser pulses. In a 1.3 cm long crystal sample pumped by 0.3 ps 515 nm laser pulses, the amplitude of $\nu_1 = 854 \text{ cm}^{-1}$ Stokes component reached 1/3 of the amplitude at the pump wavelength in the transmitted radiation spectrum. The realized energy efficiency of SRS conversion in these conditions was, however, significantly lower, below ~3.5%, and the difference was attributed to two-photon absorption (TPA) of the pump radiation [5]. TPA in CSVO crystals could also limit the pump intensity in the applications of these materials as laser media pumped by a laser with a wavelength of 0.4–0.8 μm . Therefore, the characterization of TPA in such crystals is important for their applications.

Currently, information on the TPA coefficient in CSVO can be found in two publications [5,9]. However, the coefficients they report for CSVO, $x = 0$, differ by nearly an order of magnitude, ~50 cm/TW in [5] and 250 cm/TW in [9], well beyond the measurement errors. Our analysis has shown that a possible reason for such a spread in measured TPA

Citation: Kinyaevskiy, I.O.; Kovalev, V.I.; Semin, N.S.; Danilov, P.A.; Kudryashov, S.I.; Koribut, A.V.; Dunaeva, E.E. Two-Photon Absorption in $\text{Ca}_3(\text{VO}_4)_2$ and $\text{Ca}_{2.7}\text{Sr}_{0.3}(\text{VO}_4)_2$ Crystals. *Photonics* **2023**, *10*, 466. <https://doi.org/10.3390/photonics10040466>

Received: 28 February 2023

Revised: 21 March 2023

Accepted: 8 April 2023

Published: 19 April 2023



Copyright: © 2023 by the authors. Licensee MDPI, Basel, Switzerland. This article is an open access article distributed under the terms and conditions of the Creative Commons Attribution (CC BY) license (<https://creativecommons.org/licenses/by/4.0/>).

coefficients is the difference in the irradiation regimes in [5,9]. In [5], measurements were obtained with the second harmonic radiation from a Yb-fiber laser (wavelength 515 nm) emitting 0.3 ps pulses with a 1 kHz repetition rate. In [9], the second harmonic radiation of a Nd³⁺:YLiF₄ laser (wavelength 523.5 nm) was used, which emitted a train of 25 ps pulses separated by 7.5 ns and forming a Gaussian-like, smoothly varying, envelope with ~100 ns FWHM duration. A time shift of 10 ns between maxima of the transmitted and incident envelopes was observed in [9]. This indicates a non-instantaneous nonlinear absorption process [10], which in [9] was attributed to charge-transfer transitions in the (VO₄)³⁻ ionic group excited by two-photon interband absorption. By contrast, since the pulse period in [5] was much longer than 10 ns (1 ms), such an effect was not relevant and the observed nonlinear absorption should be a consequence of the TPA process alone.

The aim of this work is the systematic study of two-photon absorption in CSVO crystals of various compositions and crystallographic orientation under the same experimental conditions using sub-picosecond laser pulses with a 1 kHz repetition rate.

2. CSVO Crystals

In our work, we investigated CSVO crystals with $x = 0$ and $x = 0.3$ grown at the Department of Laser Materials and Photonics of the General Physics Institute of RAS. The crystals were optically homogeneous; the deviation of the stoichiometric composition and other impurities in the crystals were not detected within a measurement error of 0.05 at% [2]. Anomalous birefringence does not exceed $1.3 \times 10^{-5} \text{ cm}^{-1}$. The 1.3 cm long samples were prepared with the optical c-axis parallel to the entrance and exit facets, i.e., perpendicular to the light propagation direction. Transmittance (T) spectra for these samples, using linearly polarized light with different orientations of the polarization with respect to the optical c-axis, are presented in Figure 1, together with the spectrum of the laser pulse used in the experiments described below. The dotted line in Figure 1 indicates a Fresnel reflection level calculated for refractive index $n = 1.9$ (refractive index of CSVO, $x = 0$, are 1.902 and 1.877 for ordinary and extraordinary polarizations at $\lambda \approx 0.546 \mu\text{m}$ [3]).

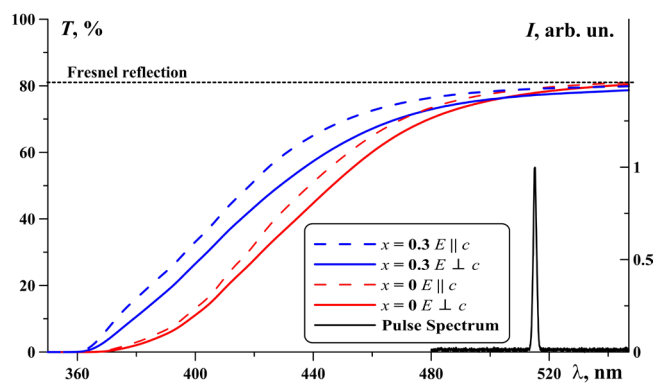


Figure 1. Transmittance spectra of CSVO crystals for $x = 0$ (red line) and $x = 0.3$ (blue line) for perpendicular (solid line) and parallel (dashed line) orientation of the light polarization and crystal c-axis. The solid black peak at 515 nm is the laser pulse spectrum.

The transparency edge for the CSVO sample at $x = 0.3$ is shifted, relative to the $x = 0$ sample, to a shorter wavelength. This is consistent with the Sr₃(VO₄)₂ energy bandgap, E_g , being higher than E_g for Ca₃(VO₄)₂ [11]. It was also found that the transmission edge depends on the crystal orientation: when the light polarization is parallel to the c-axis, E_g is slightly higher than when they are perpendicular. The estimated E_g of our samples was, respectively, ~3.38 eV and ~3.39 eV for parallel and perpendicular orientations at $x = 0$, and ~3.42 eV and ~3.43 eV for parallel and perpendicular orientations at $x = 0.3$.

3. Experiment Set-Up

The optical scheme of the TPA experiments is shown in Figure 2. The measurements were carried out with second harmonic radiation from an ytterbium fiber oscillator/amplifier laser system (Satsuma, Amplitude laser, France) emitting 0.3 ps pulses with 1 kHz repetition rate at the wavelength $\lambda = 515$ nm. Linear absorption of the laser radiation with such λ in CSVO samples was insignificant and the transmittance of the samples at low intensity was determined only by Fresnel reflection losses (see Figure 1). The laser pulse energy E_p was up to 3.2 μ J and it was varied by a polarizer-attenuator. The laser was focused into the crystal samples, using a lens with a focal length of $f_1 = 9$ cm, into a spot with a radius $\omega_0 = 26$ μ m at the $1/e^2$ level (in the focal plane). The laser operated on the fundamental TEM₀₀ mode with a Gaussian spatial profile. With the beam doubled in Rayleigh range, $2\pi n\omega_0^2/\lambda$, corresponding to 1.5 cm, the shorter sample length of $L = 1.3$ cm could be taken as the effective interaction length. The output radiation was directed to an Ophir-3A power meter or spectrometer Avesta-150 through a lens with a focal length $f_2 = 100$ mm. The angle between the linear polarization of the laser beam and the CSVO optical c-axis was set by a rotation of the sample.

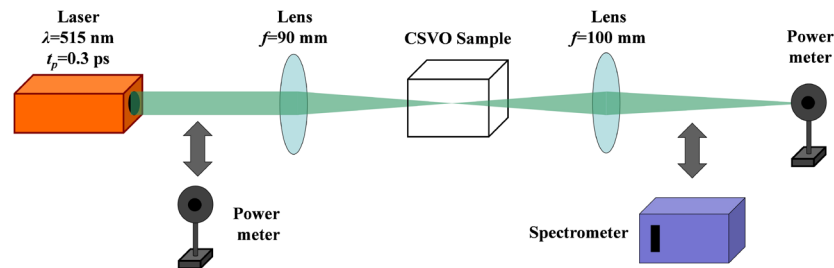


Figure 2. Optical scheme of the experiment.

4. Data Processing Procedure

The decrease in the radiation intensity due to TPA in an optically transparent material is described (without taking into account Fresnel losses) by the expression [12]:

$$I_{out} = \frac{I_{in}}{1 + \beta I_{in} L} \quad (1)$$

where I_{in} is the radiation intensity at the sample entrance, I_{out} is the radiation intensity at the exit, L is the sample length, and β is the TPA coefficient. This expression is a solution of the well-known Bouguer's equation:

$$\frac{dI}{dz} = -k_{ef} I \quad (2)$$

where k_{ef} is an effective extinction coefficient, which in our case is determined by TPA, i.e., $k_{ef} = \beta I$. Equations (1) and (2) presume the incident intensity is uniformly distributed across the laser beam and continuous in time. In reality, however, neither of these conditions are met, and, consequently, further analysis of the experiment data is required. To correctly apply Equation (1), the spatial and temporal pulse distribution must be divided into sections in which the intensity $I(r, t)$ can be assumed constant. The radiation intensity at the sample exit for each section may then be calculated using Equation (1) and the total energy of the transmitted radiation pulse E_{out} is evaluated by summing the contributions from each section. The TPA coefficient can then be obtained from the dependence on the input laser pulse energy E_p of the sample transmittance: $T = (1-R)^2 E_{out}/E_p$, where R is the Fresnel reflection coefficient of the surfaces.

Presuming the incident radiation is an axially symmetric beam with a non-uniform transverse distribution and varying in time intensity, $I_{in}(r, t) = I_0 \rho(r) \theta(t)$, where I_0 is the

maximum beam intensity and ρI and $\theta(t)$ are the functions describing the spatial distribution and temporal evolution of the intensity, E_{out} may be evaluated through substituting $I_{in}(r, t)$ into Equation (1) and integrating $I_{out}(r, t)$ over r and t :

$$E_{out} = \pi \int_{-\infty}^{\infty} dt \int_0^{\infty} I_{out}(r, t) 2r dr \quad (3)$$

The spatial distribution of the Gaussian beam is described by

$$\rho(r) = e^{-2r^2 / \omega_0^2} \quad (4)$$

where ω_0 is the beam radius at $1/e^2$ from maximum. The time-domain representation for ultrashort laser pulses is more variable [13]. For a Gaussian-shaped pulse, we have:

$$\theta(t) = e^{-t^2 / \tau^2} \quad (5)$$

where τ is the half-pulse width at the level $1/e$ from maximum (HW1/eM). For profiles Equations (4) and (5), the maximum intensity $I_0 = I(r = 0)$ and energy E_p of the laser pulse measured experimentally are related by:

$$I_0 = \frac{2E_p}{\pi\omega_0^2 t_p} = \frac{3.22E_p}{\pi\omega_0^2 \tau} \quad (6)$$

where t_p is the FWHM duration for the pulse described by Equation (5).

The spatial domain integration in Equation (3) with $\rho(r)$ described by Equation (4) gives the analytic expression:

$$\int_0^{\infty} \frac{e^{-2r^2 / \omega_0^2}}{1 + \beta I_0 L e^{-2r^2 / \omega_0^2}} 2r dr = \frac{\omega_0^2 \ln(\beta I_0 L - 1)}{2\beta I_0 L} \quad (7)$$

resulting in the expression for E_{out} :

$$E_{out} = \frac{\pi\omega_0^2}{2\beta I_0 L} \int_{-\infty}^{\infty} \frac{\ln(\beta I_0 \theta(t) L - 1)}{\theta(t)} dt \quad (8)$$

To relate this expression with the experimental data, the integration in Equation (8) for the chosen $\theta(t)$ (Equation (5)) was performed numerically.

5. Experimental Results

Unlike [5], in this work, no measurable SRS peaks appeared in the spectra of the transmitted radiation in either of the crystal samples investigated, regardless of the orientation of the laser beam polarization relative to the c-axis of the crystals or the pump energies. The only modification to the spectrum observed was its broadening around the pump wavelength, caused by a self-phase modulation effect. The broadening appeared at $E_p \sim 0.5 \mu\text{J}$ and at $E_p = 3.2 \mu\text{J}$ and its width reached $\sim 3 \text{ nm}$ at $1/e^2$ level (Figure 3). This broadening was about 3 times weaker than with tighter focusing ($f_1 = 4 \text{ cm}$) in our previous work [5].

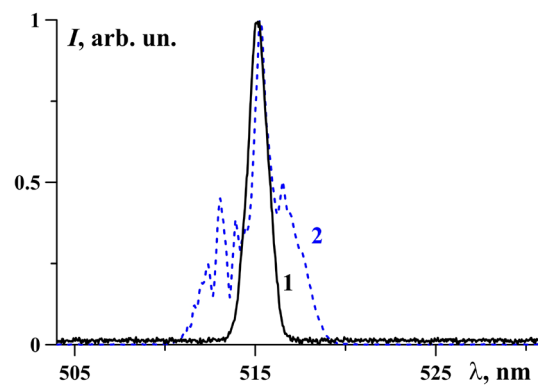


Figure 3. The spectra of laser pulse at $E_p = 3 \mu\text{J}$ at entrance (line 1) and exit (line 2) of CSVO crystal.

To evaluate β , the transmittance T of the samples was measured as a function of the incident pulse energy E_p . The experimental results for the case when the c-axis of the crystals was parallel to the laser beam polarization are presented by the points in Figure 4a. The uncertainties in measurements (Figure 4) are determined by fluctuations of input ($\pm 3\%$) and transmitted ($\pm 10\%$) pulses energy.

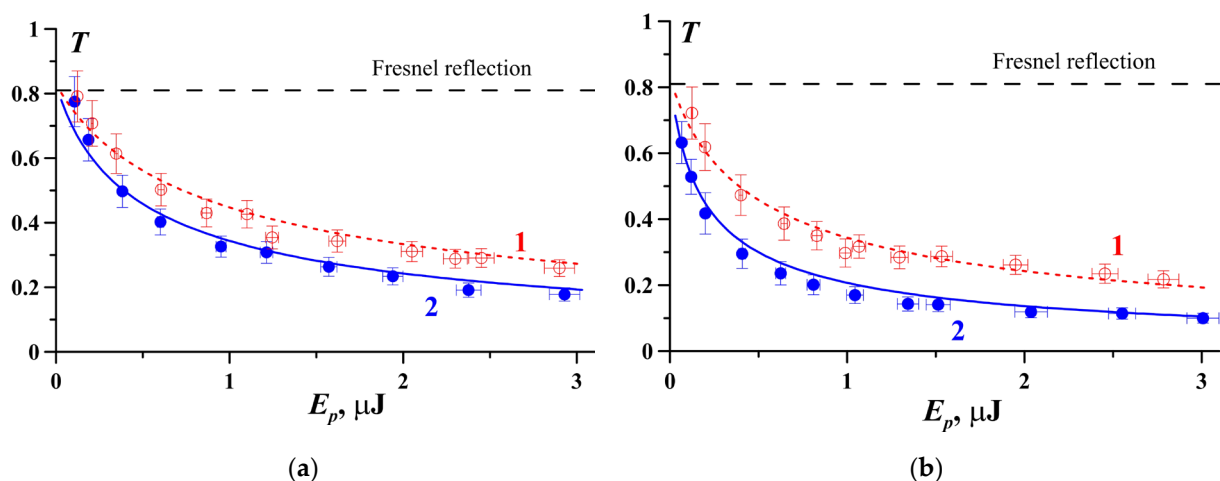


Figure 4. Dependences of the CSVO sample transmittance on the laser pulse energy for parallel (a) and perpendicular (b) orientation of the radiation polarization and the optical c-axis of the crystals; line 1: $x = 0.3$, line 2: $x = 0$.

A sharp decrease in the sample transmittance with increasing E_p is typical for TPA, as described by Equation (2). The dashed and dotted lines show the correspondent theoretical dependences calculated using Equation (8) for the magnitudes of β , providing the best fit for the experimental data. The TPA coefficients determined in this way were $19 \pm 4 \text{ cm/TW}$ and $10 \pm 2 \text{ cm/TW}$ for $x = 0$ and $x = 0.3$ CSVO crystals, respectively. Thus, the TPA coefficient for CSVO at $x = 0.3$ was ~ 2 times lower than the one for CSVO at $x = 0$.

Similar measurements and calculations were made for each crystal with the radiation polarization perpendicular to the c-axis (Figure 4b). The TPA coefficients in this case were $50 \pm 10 \text{ cm/TW}$ and $18 \pm 3 \text{ cm/TW}$ for $x = 0$ and $x = 0.3$, respectively. Thus, the ratio of TPA coefficients for $x = 0.3$ and $x = 0$ is bigger, ~ 3 times, in this perpendicular case. These magnitudes of β are consistent with those ($50 \pm 14 \text{ cm/TW}$ and $25 \pm 7 \text{ cm/TW}$) evaluated for the same samples ($x = 0$ and $x = 0.3$ CSVO) in [5], when different focusing conditions (4 cm focus lens) were used and much stronger spectral broadening of the pump radiation and notable SRS conversion took place. It should be noted that since all experimental data, herein and in [5], can be consistently described by the TPA theoretical dependence (Equation (1)), we can conclude that no other nonlinear effects affected the presented results.

The lowest TPA coefficient (~ 10 cm/TW) was observed when $x = 0.3$ and the radiation was polarized parallel to the c-axis. That was 5 times lower than for $x = 0$ with the polarization perpendicular to the c-axis. The difference in TPA coefficients for the same sample and different orientation was 2–3 times. It is known that in anisotropic media, such as the uniaxial CSVO crystal, the linear and nonlinear, including TPA, properties can depend on the crystal orientation [14]. However, the measured differences in TPA coefficients for the samples and orientations in our study cannot be explained by existing TPA theories [15,16] on the basis of differences in the energy bandgaps alone. Such a strong variation may be a consequence of a much more complicated band structure of CSVO crystals [17], the impact of which on the TPA coefficient magnitude would require more extensive theoretical consideration.

6. Conclusions

The experimentally measured TPA coefficients for $\text{Ca}_3(\text{VO}_4)_2$ and $\text{Ca}_{2.7}\text{Sr}_{0.3}(\text{VO}_4)_2$ crystals show a dependence on the concentration of Sr ions and on the orientation of the laser radiation polarization relative to the optical c-axis, but which do not correlate with the accompanying changes of bandgap. The coefficients for the perpendicular and parallel orientations were 50 ± 10 cm/TW and 19 ± 4 cm/TW in $\text{Ca}_3(\text{VO}_4)_2$ and 18 ± 3 cm/TW and 10 ± 2 cm/TW in $\text{Ca}_{2.7}\text{Sr}_{0.3}(\text{VO}_4)_2$, respectively. The measured TPA coefficient of the $\text{Ca}_3(\text{VO}_4)_2$ crystal was ~ 5 times lower, than that measured in [9], in which the effect on two-photon-induced absorption by charge-transfer transitions in $(\text{VO}_4)^{3-}$ ionic group occurred.

We highlight the following result which is important for CSVO crystal applications. To minimize optical losses due to TPA, the Sr-doped CSVO samples are preferred and the laser beam polarization should be parallel to the optical c-axis of the crystal. Low TPA coefficients and attractive SRS properties make the CSVO crystal promising for use in mid-IR laser systems, such as [18]. Higher ($>10\%$) Sr-ion concentrations may decrease TPA absorption even more; however, that should be investigated alongside the effects on other crystal properties, such as SRS [7].

Author Contributions: I.O.K.: conceptualization, investigation, writing—original draft preparation; V.I.K.: validation, numerical analysis, writing—review and editing; N.S.S.: experimental investigation, data processing, visualization; P.A.D.: experimental investigation; S.I.K.: laser setup supervision; A.V.K.: experimental investigation; E.E.D.: crystals. All authors have read and agreed to the published version of the manuscript.

Funding: This research received no external funding.

Institutional Review Board Statement: Not applicable.

Informed Consent Statement: Not applicable.

Data Availability Statement: Data underlying the results presented in this paper are not publicly available at this time but may be obtained from the authors upon reasonable request.

Conflicts of Interest: The authors declare no conflict of interest.

References

1. Chen, Z.; Wang, D.; Liu, L.; Yuan, F.; Huang, Y.; Zhang, L.; Lin, Z. Cr^{3+} doped $\text{Ca}_3(\text{VO}_4)_2$: A new tunable laser crystal. *J. Alloys Compd.* **2022**, *938*, 168651.
2. Ivleva, L.I.; Dunaeva, E.E.; Voronina, I.S.; Doroshenko, M.E.; Papashvili, A.G. $\text{Ca}_3(\text{VO}_4)_2:\text{Tm}^{3+}$ —A new crystalline medium for 2- μm lasers. *J. Cryst. Growth* **2018**, *501*, 18–21.
3. Bechthold, P.S.; Liebertz, J.; Deserno, U. Linear and nonlinear optical properties of $\text{Ca}_3(\text{VO}_4)_2$. *Opt. Commun.* **1978**, *27*, 393–398.
4. Frank, M.; Smetanin, S.N.; Jelínek, M.; Vyhlídal, D.; Ivleva, L.I.; Dunaeva, E.E.; Voronina, I.S.; Tereshchenko, D.P.; Shukshin, V.E.; Zverev, P.G.; et al. Stimulated Raman scattering in yttrium, gadolinium, and calcium orthovanadate crystals with single and combined frequency shifts under synchronous picosecond pumping for sub-picosecond or multi-wavelength generation around 1.2 μm . *Crystals* **2020**, *10*, 871.

5. Kinyaevskiy, I.O.; Kovalev, V.I.; Koribut, A.V.; Dunaeva, E.E.; Semin, N.S.; Ionin, A.A. Stimulated Raman scattering of 0.3-ps 515-nm laser pulses in $\text{Ca}_3(\text{VO}_4)_2$ and $\text{Ca}_{2.7}\text{Sr}_{0.3}(\text{VO}_4)_2$ crystals. *Opt. Spectrosc* **2023**, *131*, 207.
6. Dorbakova, N.G.; Baryshnikova, O.V.; Morozov, V.A.; Belik, A.A.; Katsuya, Y.; Tanaka, M.; Stefanovich, S.Y.; Lazoryak, B.I.; Tuning of nonlinear optical and ferroelectric properties via the cationic composition of $\text{Ca}_{9.5-1.5}\text{BixCd}(\text{VO}_4)_7$ solid solutions. *Mater. Des.* **2017**, *119*, 515–523.
7. Voronina, I.S.; Dunaeva, E.E.; Voronov, V.V.; Shukshin, V.E.; Smetanin, S.N.; Ivleva, L.I. Growth and characterization of $(\text{Ca}_{1-x}\text{Sr}_x)_3(\text{VO}_4)_2$ solid solutions: A search for the new materials for ultrafast Raman lasers. *Opt. Mater.* **2021**, *111*, 110642.
8. Li, C.; Yang, W.; Chang, Y. Raman scattering study of calcium orthovanadate crystal. *Jap. J. Appl. Phys.* **1985**, *24*, 508. <https://doi.org/10.7567/JJAPS.24S2.508>.
9. Chunaev, D.S.; Dunaeva, E.E.; Kravtsov, S.B.; Voronina, I.S.; Zverev, P.G. Two-photon Absorption in $\text{Ca}_3(\text{VO}_4)_2$ Crystal. In Proceedings of the European Conference on Lasers and Electro-Optics 2021, Munich, Germany, 21–25 June 2021; p. ce_p_12.
10. Kovalev, V.I.; Rus'kin, O.L.; Suvorov, M.B. Nonlinear absorption of randomly pulsating CO_2 laser radiation in narrow-gap semiconductors. *Sov. J. Quantum Electron.* **1991**, *21*, 1346.
11. Parhi, P.; Manivannan, V.; Kohli, S.; Mccurdy, P. Synthesis and characterization of $\text{M}_3\text{V}_2\text{O}_8$ ($\text{M} = \text{Ca}, \text{Sr}$ and Ba) by a solid-state metathesis approach. *Bull. Mater. Sci.* **2008**, *31*, 885.
12. Shen, Y.R. *The Principles of Nonlinear Optics*; Wiley: New York, NY, USA, 1984.
13. Von der Linde, D. Experimental study of single picosecond light pulses. *IEEE J. Quantum Electron.* **1972**, *8*, 328.
14. Bredikhin, V.I.; Galanin, M.D.; Genkin, V.N. Two-photon absorption and spectroscopy. *Sov. Phys. Usp.* **1973**, *16*, 299–321.
15. Keldysh, L.V. Ionization in the field of a strong electromagnetic wave. *Sov. Phys. JETP* **1965**, *20*, 1307.
16. Basov, N.G.; Grasyuk, A.Z.; Zubarev, I.G.; Katulin, V.A.; Krokhin, O.N. Semiconductor quantum generator with two-photon optical excitation. *Sov. Phys. JETP* **1966**, *23*, 366.
17. Logvinov, I.N.; Perel'man, N.F. Theory of many-photon transitions in insulating crystals. *Sov. Phys.-Solid State* **1980**, *22*, 372.
18. Kinyaevskiy, I.O.; Koribut, A.V.; Grudtsyn, Y.V.; Seleznev, L.V.; Kovalev, V.I.; Pushkarev, D.V.; Dunaeva, E.E.; Ionin, A.A. Frequency down-conversion of a chirped Ti: Sapphire laser pulse with BaWO_4 Raman shifter and second-order nonlinear crystal. *Laser Phys. Lett.* **2022**, *19*, 095403.

Disclaimer/Publisher's Note: The statements, opinions and data contained in all publications are solely those of the individual author(s) and contributor(s) and not of MDPI and/or the editor(s). MDPI and/or the editor(s) disclaim responsibility for any injury to people or property resulting from any ideas, methods, instructions or products referred to in the content.